Static and dynamic properties of the structural phase transitions in NaNbO₃

A. Avogadro, G. Bonera, F. Borsa, and A. Rigamonti

Istituto di Fisica dell'Università di Pavia, and Unità di Pavia del Gruppo Nazionale di Struttura della Materia Consiglio Nazionale delle Ricerche, 27100 Pavia, Italy

The static and dynamic properties which characterize the structural phase transitions in NaNbO₃ have been widely investigated by transient NMR measurements of the Na^{23} and Nb^{93} nuclei in a powdered sample (no large-enough single crystal was available). The temperature range investigated (100–1100 °K) includes both the purely structural transitions associated with the tilting of the NbO_6 octahedra and the ferroelectric and antiferroelectric transitions associated with the off-center motion of the Nb atoms. The static effects have been investigated through the changes in the free-precession decay of the central line due to second-order quadrupole broadening. The dephasing time of the free-precession decay has been related to the quadrupole coupling constant. The temperature dependence of the rotational displacement of the NbO_6 octahedra and of the off-center displacement of the Nb ions is then obtained. The variation of the tilt angle φ of the oxygen octahedra near the transition at 641 °C is very rapid and it is not possible to decide whether φ goes to zero continuously or with a small discontinuity. The maximum value of φ in the tetragonal phase, as deduced from a crude estimate of the electric field gradient in a point-charge model, is about 7°. No off-center displacement of the Nb atom is observed, on cooling, before the 480 °C transition. The numerical values for the Nb displacements in the R and P phase (≈ 0.11 Å at 373 °C and ≈ 0.15 Å at 315 °C) are in good agreement with previous indications of x-ray diffraction measurements. The dynamic effects have been investigated through nuclear spin-lattice quadrupole relaxation. A theory is developed which relates the relaxation rate to the critical parameters of the central peak in the dynamic cubic-tetragonal phase transition at 641 °C, a value $v \simeq 0.6$ for the critical index of the correlation length can be estimated; the rotational fluctuations appear to have a quasiplanar correlation. The experimental results seem to indicate that for $(T - T_c) \approx 4$ °C the slowing down reaches an angular frequency of the order of 300 MHz. Finally, an estimate for the root-mean-square local fluctuating angle near T_c of about 1.6° is obtained.

I. INTRODUCTION

Sodium niobate is a crystal belonging to the perovskite family of general formula ABX_3. In this family the basic unit of the ideal structure consists of corner-linked regular octahedra of X anions (usually oxygen) with B cations in their center and A cations at the corner of a simple cubic lattice enclosing the octahedron.[1] These materials have attracted a considerable interest because of their important properties such as ferroelectric and antiferroelectricity, piezoelectricity, and nonlinear optical behavior; they are characterized by a variety of structural phase transitions associated with small distortions from the ideal cubic structure. The cubic structure is found in some crystals such as $SrTiO_3$ and $KMnF_3$ at room temperature, while in others such as $NaNbO_3$, $LaAlO_3$, and $KNbO_3$, only at very high temperatures. The observed distortions usually involve one or more tilts of the rigid octahedron around its symmetry axis, sometimes accompanied by a small distortion of the octahedron itself; the antiferroelectric and ferroelectric transitions are furthermore linked with the displacements of the cations.[2] Following Glazer and Megaw,[1,2] we classify the different tilted systems of the rigid octahedra with the symbol

$$a^{(i)} b^{(j)} c^{(k)} \quad ,$$

where a, b, c indicate tilts around one of the pseudocubic axes (the letters themselves indicate equality or inequality of their magnitudes), while i, j, k are relative to the sense of the tilt of successive octahedra along an axis: the same (+), opposite (−), or no tilt (0).

Sodium niobate exhibits an entire series of structural transitions involving different types of tilts of the octahedra and displacements of the cations. This justifies the considerable effort spent in recent years in investigating this crystal by x rays at various temperatures.[3-6] As a result, the temperatures of the transitions and the symmetry of the phases have been rather well established.

Nuclear magnetic resonance is a useful tool to investigate the static and dynamic effects near structural phase transitions on a microscopic scale and $NaNbO_3$ is a particularly suitable crystal, since both Na^{23} and Nb^{93} nuclei ($I = \frac{3}{2}$ and $I = \frac{9}{2}$, respectively) can be utilized as probes of the structural changes and of the critical fluctuations through their coupling with the crystalline electric field gradients (efg). The subsequent atomic displacements from the equilibrium positions occupied in the high-temperature cubic phase (above 641 °C) can be determined as a function of temperature from the measurements of the static quadrupole effects on the NMR spectrum, while the fluctuations in the critical variables (tilt angles,

displacement of cations) in the neighborhood of the phase transitions can be investigated by quadrupole spin-lattice relaxation measurements. At present, the only study of $NaNbO_3$ by NMR is an investigation of the static quadrupole effects by continuous-wave technique in a powdered sample in the ferroelectric and antiferroelectric phase from -170 to $270\,°C$.[7]

The growth of a single crystal large enough for NMR is very difficult, and therefore the present work also had to be performed on a powder. However, the aim of the present investigation is to study in particular the high-temperature phase transitions where the lattice distortions are simpler and consequently a large amount of information can be obtained even on a powder, as it will be shown in the coming sections.

Regarding the static effects, the effort is concentrated in determining the temperature dependence of the rotational order parameter at the cubic-tetragonal phase transition which involves tilts of the type $a^0a^0c^+$ and in investigating the off-center displacements of Nb at the phase transitions at $480\,°C$ $(a^-b^+c^+ \rightarrow a^-b^0c^+)$ and at the antiferroelectric transition at $373\,°C$. The results are reported in Secs. IIIA and IIIB, respectively. Regarding the dynamic effects, the nuclear spin-lattice relaxation measurements reported in Sec. IV are helpful in determining the properties of the soft-phonon modes involved at each transition. Preliminary results on this subject have been published[8] and it was mentioned that the softening of the whole branch from the R point $\vec{q} \equiv (1/a)(\pi, \pi, \pi)$ to the M point $\vec{q} \equiv (1/a)(\pi, \pi, 0)$ accounts for the remarkable two-dimensional character of the fluctuation of the rotation angle of the oxygen octahedra. Information about the dynamics of the critical fluctuations are also to be obtained and interpreted in the light of the recent findings about a central component at zero frequency of the soft mode.

Section II, devoted to the experimental details, is developed in some length, since it was necessary to make a rather elaborate analysis of the experimental data, particularly of the free-precession (fp) decays, in order to extract the relevant parameters.

II. EXPERIMENTAL DETAILS AND ANALYSIS OF DATA

A. Experimental

The Na^{23} and Nb^{93} nuclear magnetic resonances were studied by pulse techniques with a Brüker B-KR 306 coherent pulse spectrometer operating at 22 MHz. The maximum intensity available for the rf field H_1 was 20 Oe. The transient nuclear signal was recorded by a box-car integrator or by a 200-channel fast signal averager with a maxi-

mum resolution of 2 μsec per channel. In order to avoid the nonlinearity due to the diode detection, the measurements were usually performed in heterodyne mode. The temperature range explored was $80-1100\,°K$. The high-temperature measurements were performed with a water-cooled furnace heated by a "thermocoax" coil, whose current was controlled by a feedback system driven by the thermocouple in the sample. While the temperature stability was better than $0.1\,°C/h$, temperature gradients of about $1\,°C/cm$ could not be eliminated at the highest temperatures. Near the high transition point $(641\,°C)$ it was therefore necessary to use a very small sample, reaching the limit of the observability of the signal at the oscilloscope.

B. Samples

The investigation was carried out in two different samples which we will refer to as samples I and II. Sample I was in the form of fine powder and it was purchased from Alfa Inorganics Inc. The preliminary measurements were performed in this sample and from a careful investigation of the temperature region around the $641\,°C$ transition, two anomalous peaks appeared in the nuclear relaxation rate.[9] Measurements of differential thermal analysis (DTA) performed on sample I confirmed that the anomalous behavior observed in the relaxation rate was due to what appears to be an extra phase transition at about $660\,°C$ (see Fig. 1). Sample II was a collection of small single crystals kindly given to us by Glazer. The DTA of sample II and the nuclear relaxation rate display only a single anomalous rising around $641\,°C$ (see subsection D).

C. Free-precession analysis

The structural variations associated to the phase transitions and, in particular, the temperature dependence of the tilting angle of NbO_6 octahedra
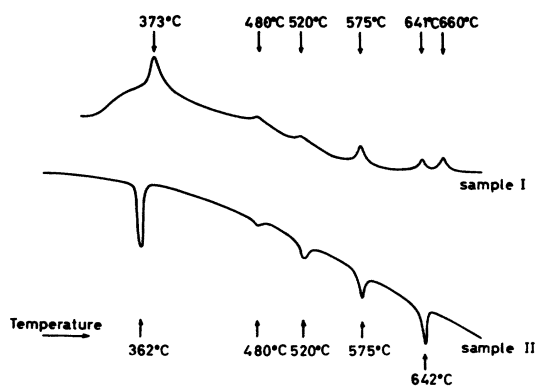

FIG. 1. Differential thermal analysis of the polycrystalline samples I and II of $NaNbO_3$.

and the off-center displacements of the Nb atom have been investigated through the static quadrupole effects on the Na^{23} and the Nb^{93} resonance spectra. Unfortunately this type of study is in general less reliable in a powder than in a single crystal; in fact, while in a single crystal a static efg produces, in first order, a shift of the satellite lines and, in second order, a shift of the central line, in a powder it produces a broadening of the resonance spectrum, and in practice only the second-order broadening of the central line can be studied. For the high-temperature transitions we have investigated this broadening with pulse techniques through the analysis of the fp decay. This approach has already been proved, [10] in similar cases, more reliable than that with continuous wave techniques.

The fp decay following a 90° pulse, with a strong rf field H_1, yields the Fourier transform of the frequency-distribution spectrum. In the assumption of a Gaussian distribution the shape of the fp decay is $h(t) \propto e^{-t^2/\tau^2}$ where the dephasing time τ is related to the second moment M_2 of the distribution by the equation

$$M_2^{1/2} = (\pi \sqrt{2} \, \tau)^{-1} \quad . \tag{1}$$

In the cubic high-temperature phase the broadening of the resonance line is due to the nuclear dipolar interaction and the second moment can be evaluated by the Van Vleck formula. One obtains for Na^{23} and Nb^{93}, respectively,

$$\begin{aligned} Na^{23}: \quad & M_2 = (0.325 + 2.12) \text{ kHz}^2 = (1.57 \text{ kHz})^2, \\ Nb^{93}: \quad & M_2 = (1.8 + 0.33) \text{ kHz}^2 = (1.45 \text{ kHz})^2, \end{aligned} \tag{2}$$

where the first contribution is from like nuclei and the second one from unlike nuclei. In the case of Na^{23} the line broadening is due mostly to the dipolar interaction with unlike spins. Since $\gamma_{Na23} \simeq \gamma_{Nb93}$, no line-narrowing effects due to unlike spins flipping[11] is present and the line shape should still be Gaussian, so that Eq. (1) is valid.

In the distorted phases an extra broadening arises from the quadrupole interaction with the static efg. The satellite lines $m \rightarrow m-1$ are spread over a frequency range of about $2\nu_Q(m - \frac{1}{2})$, where $\nu_Q = 3eQV_{zz}/2I(2I-1)h$ and V_{zz} is the greatest component of the efg tensor in the principal axis frame of reference Σ^P. A theoretical calculation was performed in the case of an axially symmetric efg. For $I = \frac{3}{2}$ it was found that the contribution to the fp signal coming from satellite transitions (60% of the signal if all lines are irradiated), reduces to e^{-1} in a time $\tau \simeq \frac{1}{2}\nu_Q$ and shows beats after a long time whose maximum height is approximately 20% of the total satellite contribution. For $I = \frac{9}{2}$, on the other hand, the contribution from the satellite transitions (85% of the signal) is practically

given in a short time period by a Gaussian decay with a dephasing time $\tau \simeq 0.225/\nu_Q$. For an indicative value for ν_Q of 100 kHz the contribution to the fp decay arising from the satellite transitions is not observable because it decays during the dead time of the receiver (~ 10 μsec). In the presence of second-order effects the central line is spread out over a frequency range of about $[I(I+1) - \frac{3}{4}]\nu_Q^2/3\nu_L$ and its second moment due to the dipolar interaction between like spins is modified by a factor $\xi = 0.9$ for Na^{23} and $\xi = 1.3$ for Nb^{93}.[12] In particular the fp decay of the central line, due solely to the quadrupole broadening and detected in quadrature with the rf field, can be written

$$h_x(t) \propto \int \cos\left[2\pi\nu_{1/2}^{(2)}(\vartheta, \varphi, \eta)t\right] d(\cos\vartheta) \, d\varphi \quad , \tag{3}$$

where the second-order quadrupole shift for the central line $\nu_{1/2}^{(2)}(\vartheta, \varphi, \eta)$ depends on the orientation of Σ^P with respect to the frame of reference of the magnetic field Σ^H, and from the asymmetry parameter $\eta = |V_{xx} - V_{yy}|/V_{zz}$.

In Fig. 2(a) the fp decays obtained through numerical integration of Eq. (3) for $\eta = 0$ and $\eta = 1$ are reported. Since the second-order quadrupole broadening is not symmetrical with respect to the Larmor frequency ν_L, a small in-phase signal is also present. As it can be seen from Fig. 2(b), the fp decay is practically Gaussian with a dephasing time τ_Q given by the relations

$$\tau_Q = 3R_\eta \, \nu_L/\pi\left[I(I+1) - \frac{3}{4}\right]\nu_Q^2 \quad , \tag{4}$$

where $R_\eta = 3.05$ for $\eta = 0$ and $R_\eta = 2.65$ for $\eta = 1$. Therefore, when both dipolar and quadrupole broadening are present we can assume for the effective dephasing time for the fp decay of the central line the following expression:
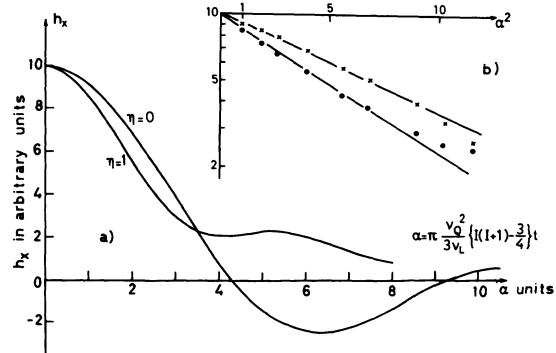

FIG. 2. (a) Theoretical fp decay $h_x(t)$, detected in quadrature with the rf field, for the central line in presence of a second-order quadrupole broadening in powder and for the two extreme values of the efg asymmetric parameter η. (b) Gaussian plot of the fp decays.
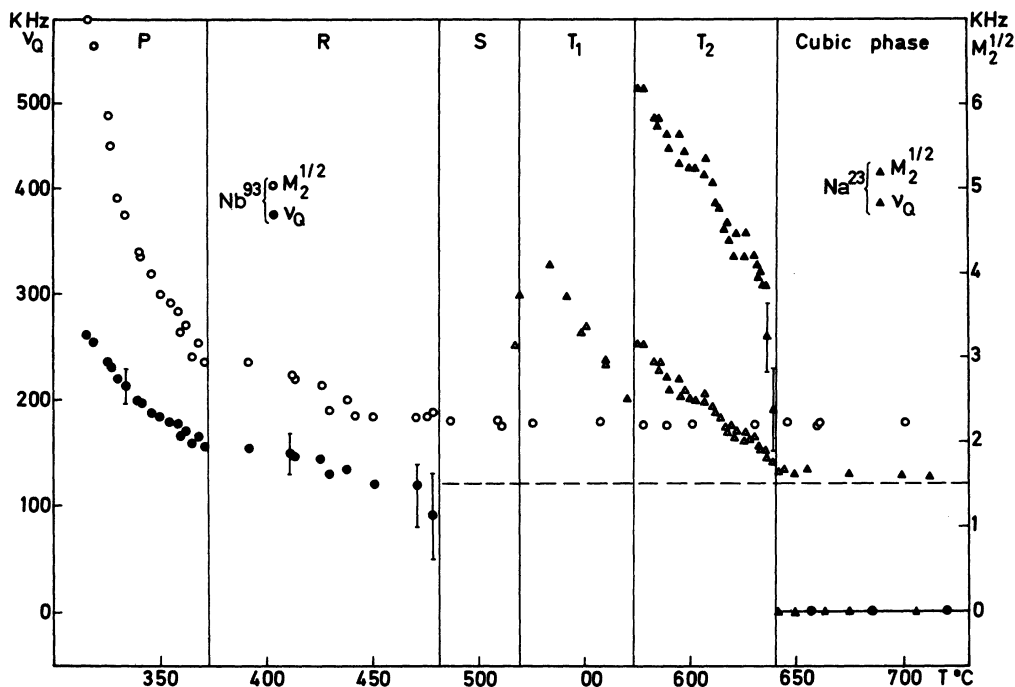
FIG. 3. Square-root values $M_2^{1/2}$ of the second moment for the Na[23] and Nb[93] resonance line and quadrupole frequency ν_Q as a function of the temperature.

$$1/\tau^2 = 1/\tau_Q^2 + 2\pi^2 \xi' M_2 \quad .$$

Then from Eq. (4),

$$\nu_Q = \{3\sqrt{2} R_n \nu_L / [I(I+1) - \tfrac{3}{4}]\}^{1/2} (M_2^* - \xi' M_2)^{1/4} \quad , \quad (5)$$

where $M^* = \tfrac{1}{2}\pi^2 \tau^2$ can be considered as a "second moment" of the quadrupole broadened central line.

It should be observed that the fp decay is truly the Fourier transform of the resonance frequency distribution only if $(1/2\pi)\gamma H_1 \gg (M_2^*)^{1/2}$; this condition is not well verified, particularly in the distorted phases, as can be seen by comparing the experimental values of $(M_2^*)^{1/2}$ reported in Fig. 3 with the experimental value of $(1/2\pi)\gamma H_1 \simeq 20$ kHz. From a study of the effects of the rf field intensity on the fp shape (see Appendix A) one can infer that for $(M_2^*)^{1/2} \lesssim \tfrac{1}{2}(1/2\pi)\gamma H_1$ the fp signal is again the Fourier transform of the frequency distribution, provided that a translation in the origin of the time is made by a quantity $t_1 = \tfrac{1}{4}\pi(\gamma H_1)^{-1}$ for dipolar broadening by like nuclei and of the quantity $t_1 = (\gamma H_1)^{-1}$ for dipolar broadening by unlike nuclei or for a broadening by second order quadrupole interaction.

In Fig. 3 the square root of the second moment as obtained from the dephasing time of the fp decay by taking into account the time-translation correction, is reported for Na[23] and Nb[93] in the temperature range 300–750 °C.

In the cubic phase the experimental second mo-

ment for the Na[23] $[(M_2^*)^{1/2} = 1.6$ kHz] is in good agreement with the Van Vleck theoretical value. For temperatures a few degrees below 641 °C a marked decrease in the intensity of the fp decay occurs which corresponds to the complete smearing out of the satellite lines due to the tilting $a^0 b^0 c^*$ of the oxygen octahedra.

For Nb[93] in the cubic phase, the fp shows a fast decaying component at short times and a Gaussian slowly decaying component from which the second moments reported in Fig. 3 were obtained. The fast decaying component should be due to a partial
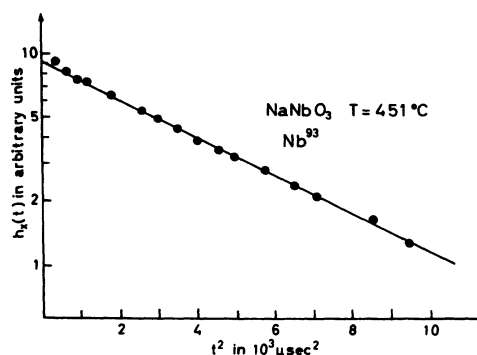

FIG. 4. Gaussian plot of the experimental Nb[93] fp signal at $T = 451$ °C.

spreading out of the satellite lines associated to the presence of strains or crystalline defects; a small satellite echo can in fact be detected in the cubic phase. The second moment is almost 50% greater than the theoretical Van Vleck value. This difference, however, is not relevant in view of the possible presence for Nb^{93} of other sources of broadening and of the uncertainty in the experimental evaluation. It should be observed that this uncertainty does not affect the deduced temperature behavior of the static efg, since at the temperature at which a second-order extra broadening becomes detectable, the satellite lines are completely smeared out and the fp decay is Gaussian, as indicated in Fig. 4.

In Fig. 3 are also reported the quadrupole frequency ν_Q obtained from Eq. (5). For Na^{23} in the tetragonal T_2 phase, it was assumed $\eta = 1$, and for Nb^{93} in the antiferroelectric R and P phases it was assumed $\eta = 0$ and $\eta = 0.33$, respectively (see Sec. III).

It should be stressed that a large error in the value of ν_Q is present for the temperature range in which the second-order quadrupole extra broadening of the central line is small with respect to the dipolar linewidth. Moreover, in this range a further difficulty in the analysis of the data is due to the progressive first-order quadrupole broadening of the satellite lines and the simultaneous changeover of the dipolar second moment.

The Nb^{93} second moment does not exhibit any appreciable change at the 641, 575, and 520 °C phase transitions, indicating that until 480 °C the static efg should be small; this is in agreement with the fact that, as indicated in Sec. III, the efg at Nb site associated to the small tetragonal distortion and to the tiltings $a^0 a^0 c^+$, $a^- b^0 c^+$, $a^- b^+ c^+$ are not detectable.

D. Spin-lattice relaxation measurements

The Na^{23} and Nb^{93} spin-lattice relaxation has been investigated by applying a saturating comb of about twenty 90° pulses (in a time long with respect to the dipolar dephasing time and short with respect to the spin-lattice relaxation times) and by detecting after a time t the height $s(t)$ of the fp signal following a further 90° pulse. When the signal was strongly-broadened by second-order quadrupole effects, the measurements were made on the echo following a pair of 90° pulses.

In the high-temperature cubic phase, where the Zeeman levels are equally spaced, and in the spin-temperature hypothesis, the recovery law for Na^{23} is

$$[s(\infty) - s(t)]/s(\infty) = e^{-2(W_1 + 4W_2)t/5} , \qquad (6)$$

where W_1 and W_2 are the $\Delta m = 1$ and $\Delta m = 2$ relaxation transition probabilities induced by the time-dependent quadrupole interaction.

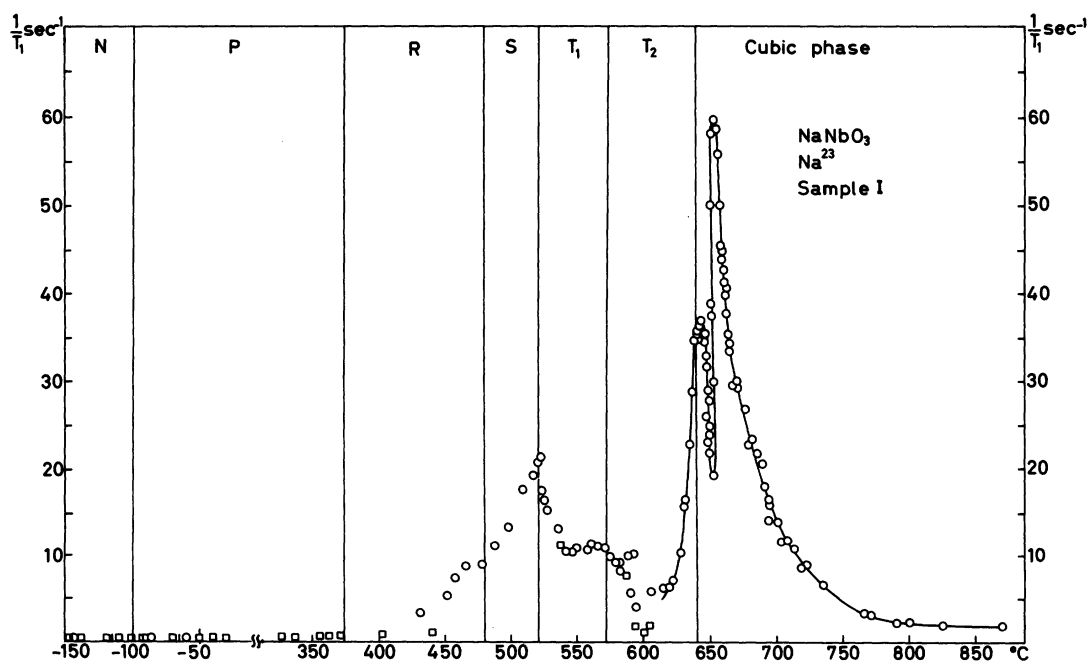In the distorted phases ($T \leq 540$ °C), where prac-

FIG. 5. Temperature behavior of the Na^{23} relaxation rate in sample I. The data indicated by □ refer to measurements performed on the echo signal.
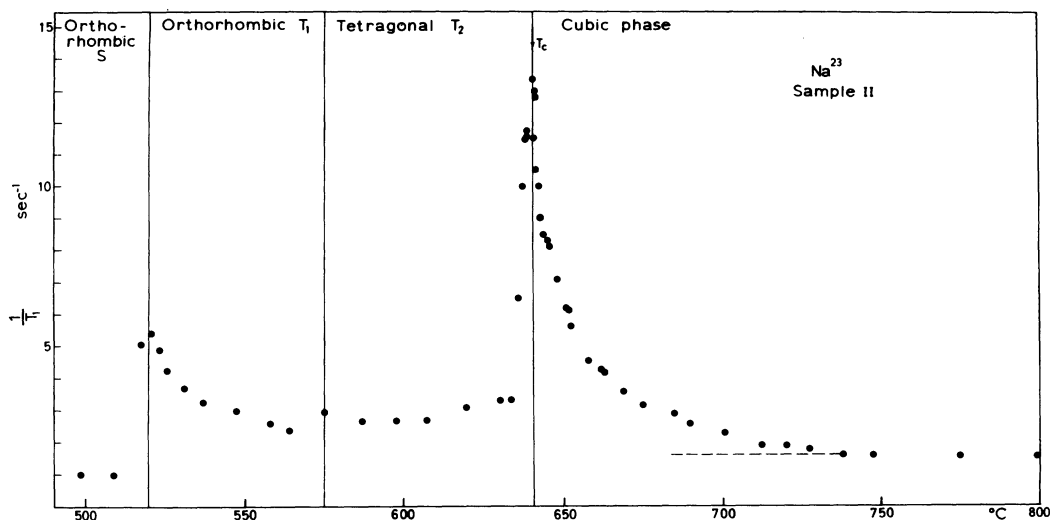
FIG. 6. Temperature behavior of the Na^{23} relaxation rate in sample II.

tically only the Na^{23} central line is irradiated and detected, the recovery law is

$$[s(\infty) - s(t)]/s(\infty) = \tfrac{1}{2} e^{-(2W_1)t} + \tfrac{1}{2} e^{-(2W_2)t} \quad . \quad (7)$$

Just below 641 °C, where the progressive spreading out of the Na^{23} satellite lines occurs, the recovery law changes in a complicated way from Eq. (6) towards Eq. (7). However, since the experimental recovery plot at any temperature is almost exponential, W_1 and W_2 should be of the same order of magnitude: in this case the two recovery laws are practically the same, yielding an exponential recovery with a time constant $1/T_1 = 2W$.

The static efg at Nb^{93} should be small also in the distorted phases for temperatures greater than

480 °C, and the quadrupole spin-lattice recovery law should be given by

$$[s(\infty) - s(t)]/s(\infty) = e^{-(1/15)(W_1 + 4W_2)t} \quad , \quad (8)$$

where $W_1 = 6W_{3/2 \cdot 1/2}$ and $W_2 = \tfrac{24}{25} W_{3/2 \cdot 1/2}$.

For $T \le 480$ °C, where a sizeable second-order static efg is present, one irradiates and detects only the central line and the recovery law is[13]

$$[s(\infty) - s(t)]/s(\infty) = \tfrac{1}{2} e^{-[(25/12)W_2]t}$$

$$+ \tfrac{1}{2} e^{-[(1/3)W_1 + (21/24)W_2]t} \quad . \quad (9)$$

In this case, even if one assumes $W_1 = W_2 = W$, the recovery law is not exponential; however, since the ratio of the two time constants in Eq. (9) is
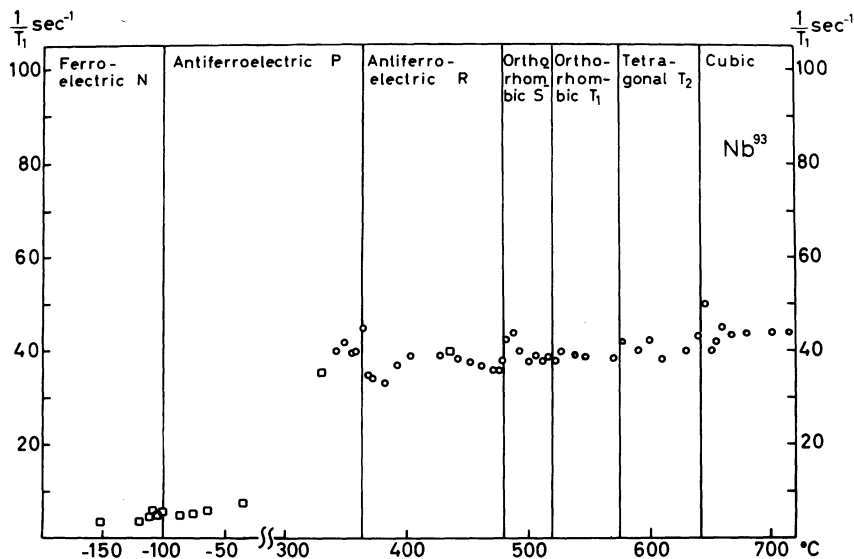

FIG. 7. Temperature behavior of the Nb^{93} relaxation rate. The results indicated by □ refer to measurements performed on the echo signal.

less than 2, it is difficult to separate from the recovery plot the two exponentials, and one practically measures an average time constant $1/T_1 = \frac{79}{48} W$. For all lines superimposed and with the assumption that $W_1 = W_2$, one has $1/T_1 = \frac{1}{3} W$ [see Eq. (8)].

It should be observed that also in the distorted phases it is possible to obtain[13] an exponential recovery for both the Na^{23} and Nb^{93} central line by irradiating with a 90° pulse sequence for a time long with respect to the spin lattice relaxation times.

The experimental results of the relaxation rates for Na^{23} and Nb^{93} are reported in Figs. 5–7. Figure 5 refers to sample I and shows the extra peak in the Na^{23} relaxation rate at the same temperature $[(660 \pm 1)\,°C]$ at which it was observed in the DTA measurements (see Fig. 1); Fig. 6 refers to sample II and only the Na^{23} relaxation rates for the range 500–800 °C are reported. The relaxation rates obtained for sample I and sample II are the same below 500 °C for Na^{23} and over the whole temperature range for Nb^{93}. The difference in behavior of the Na^{23} relaxation rate around the 641 °C transition temperature in sample I and sample II is impressive and not trivial, since a similar effect has been observed also for $NaTaO_3$.[9] The extra phase transition in the powder sample could be an interesting effect related to the surface and/or impurity content and is presently under further investigation.[14] Since sample II consists of small single crystals on which the x-ray investigation has been carried out,[4,5] we will discuss in Sec. IV B the Na^{23} measurements by referring to the results obtained in sample II.

III. STATIC EFFECTS

In this section we present and discuss the information that can be deduced from the temperature behavior of the static efg at the Na and Nb sites obtained from the analysis of the fp decay as described in Sec. II C.

A. Tilt angle of the NbO_6 octahedra for $T < 641°C$

There is evidence from x-ray measurements[4,5] that the cubic-tetragonal phase transition at 641 °C is associated with a tilting of the NbO_6 rigid octahedra that takes place in the same sense in different $(0, 0, 1)$ planes $(a^0 a^0 a^0 \rightarrow a^0 a^0 c^+)$. In addition to the tilting there is a tetragonal distortion of the cell; the distortion is related to the tilting angle approximately as[5]

$$a/c = \cos\varphi \simeq 1 - \tfrac{1}{2} \varphi^2 \quad .$$

If one computes the components of the efg tensor at the Na site, taking into account only the displacements of the nearest-neighbor oxygen, sodium, and niobium atoms, one finds in a point-charge model

$$V_{zz} = [2e(1 - \gamma_\infty)/a^3](6\sqrt{2}\,\varphi + 6.6\,\varphi^2)$$

and

$$\eta = 1 - 1.6\varphi \quad ,$$

from which

$$\nu_Q = eQV_{zz}/2h = 3.45\varphi + 2.67\varphi^2 \text{ MHz} \qquad (10)$$

(φ in rad). Writing Eq. (10) we have assumed the value of the lattice parameter of the pseudocubic cell as $a = 3.94$ Å, the antishielding factor as $\gamma_\infty = -4.8$ and $Q = 0.12 \times 10^{-24}$ cm^2.

From Eq. (10) and the data for the quadrupole frequency of Na^{23} reported in Fig. 3, one obtains the temperature dependence of the generalized order parameter φ.

In Fig. 8 the values for φ are reported as a function of $\epsilon = (T_c - T)/T_c$ for the tetragonal T_2 phase. Also in Fig. 8 the value of φ deduced from x-ray measurements[5] is also plotted for comparison. The temperature behavior deduced from NMR and x-ray measurements is similar, while there appears to be a disagreement in the absolute value of the rotation angle. However, both the absolute determinations can have a systematic error of as much as 50%. In particular, regarding NMR data, the evaluation of φ from ν_Q requires some assumptions regarding the origin of the efg (in our case we have assumed the ionic model) and the value of γ_∞. These uncertainties however, do not affect the relative temperature dependence of the angle.

As it appears from Fig. 8, the variation of φ in the neighborhood of T_c is very rapid, and it is not possible to decide whether the tilt angle goes to zero continuously or with a small discontinuity. Another difficulty in fitting the data arises from the small temperature range in which the tetragonal T_2 phase exists, which allows measurements to be done only for $\epsilon < 0.1$. If one assumes a continuous transition with $T_0 = T_c = 914$ °K, a least-squares fit yields for the temperature behavior of φ the power law

$$\varphi \propto \epsilon^{0.13 \pm 0.05} \quad , \qquad (11)$$

with a very low value of the critical exponent β, very different from the value 0.5 which holds in the framework of the mean-field approximation and Landau theory. Another way to fit the experimental results is to fix the value of β and to leave T_0 as best-fit parameter. With $\beta = \frac{1}{2}$ one obtains a good fit with $T_0 \sim 947$ °K; this would imply a weakly first-order transition. By setting $\beta = \frac{1}{3}$ (as found through very accurate EPR measurements by Müller and Berlinger[15] in $SrTiO_3$ and $LaAlO_3$ in the same range of the reduced temperature) one obtains $T_0 = 926$ °K; this value still implies a weakly first-order transition, with nonclassical critical effects as found in $KMnF_3$.[16]

It should be observed that even for a quasicontinuous phase transition a small discontinuity in the temperature behavior of φ should always take place; in fact, as argued by Glazer and Megaw[4] from symmetry considerations, the minimum value that φ can assume in the distorted phase must be at least greater than the rms value of the fluctuations of the angle itself.

B. Off-center displacement of Nb

The measurements of quadrupole coupling constant of the Nb^{93} do not give information about the tilting of the oxygen octahedra. From the experimental results in Fig. 3, it can be seen that no measurable quadrupole broadening of the Nb central line occurs for $T > 480\,°C$. This means that the quadrupole coupling constant ν_Q remains lower than about 70–80 kHz. This fact can be justified even with a crude estimate of the static efg at the Nb site due to the tilting of the octahedra and the consequent tetragonal distortion; in a point-charge approximation one obtains for the contribution of the nearest-neighbor oxygens

$$V_{zz} = [2e(1 - \gamma_\infty)/a^3]\{48\,\varphi^2 - 32\,[1 - (a/c)^3]\} \quad .$$

By using the relation $a/c = \cos\varphi$, one finds that the two contributions, which are small anyway, cancel each other.

On the other hand, an appreciable efg can arise at the Nb site if the ion itself moves off-center in the rigid NbO_6 octahedra. Referring to Fig. 3, we can conclude that the rapid increase of ν_Q in phase R, and more so in phase P, are to be related to the antiferroelectric off-center motion of the Nb ion. Let us assume that in the phase R the Nb is displaced by an average amount δ in the [100] direction.[17] The fact that in different cells the displacement has opposite sign does not matter, since we are sensitive only to the absolute value of the efg. The contribution to the efg at the Nb site, due to the oxygens belonging to the NbO_6 octahedra, is given in the point-charge approximation by

$$V_{zz} = 1344\,[2e(1 - \gamma_\infty)/a^3]\,(\delta/a)^2 \quad \text{and} \quad \eta = 0 \quad .$$

The quadrupole coupling frequency is then

$$\nu_Q \simeq 260\,(\delta/a)^2 \text{ MHz} \quad . \tag{12}$$

From Eq. (12) and the data in Fig. 3, one deduces that the average off-center displacement of Nb in phase R begins at 480° and, on cooling, reaches a value of about 0.1 Å at the transition temperature of 375 °C.

Phase P, which is also antiferroelectric, is characterized by an off-center displacement of Nb by an amount λ in the [101] direction. Under the same simplifications as before, the static efg is given by

$$V_{zz} = 1008\,[2e(1 - \gamma_\infty)/a^3]\,(\lambda/a)^2 \quad \text{and} \quad \eta = \tfrac{1}{3} \quad .$$

The corresponding quadrupole coupling frequency is

$$\nu_Q = 195\,(\lambda/a)^2 \text{ MHz} \quad . \tag{13}$$
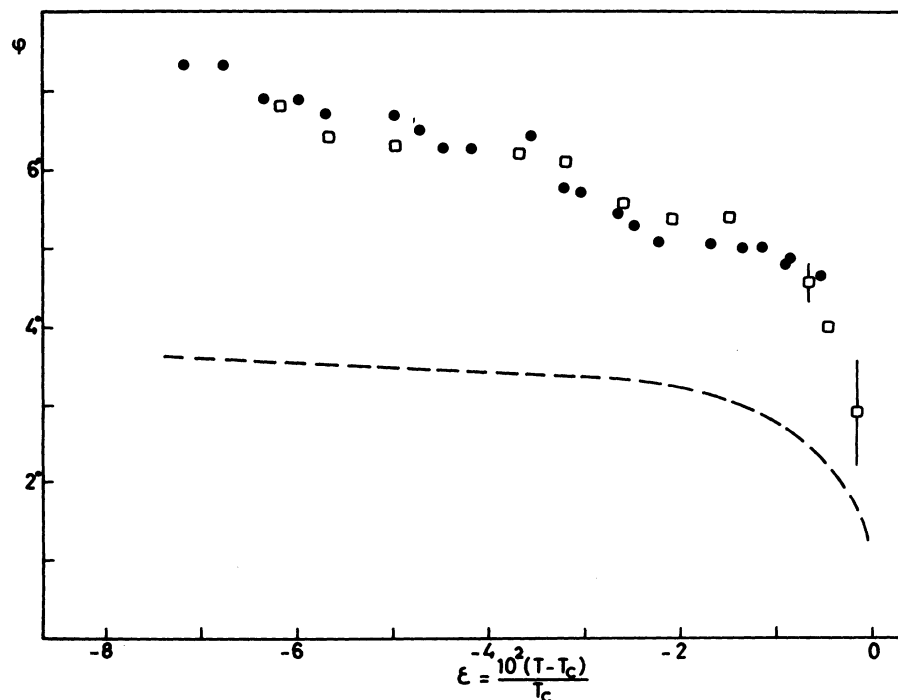

FIG. 8. Tilt angle for the oxygen octahedra as a function of $\epsilon = 10^2 \times (T - T_c)/T_c$ with $T_c = 914\,°K$. The data indicated by ● refer to sample I and the data indicated by □ to sample II. The dotted line represents an indicative behavior of the values obtained from x-ray diffraction (see Ref. 5).

In light of Eqs. (12) and (13) the absence of a sizeable variation in the experimental values of ν_Q at the R-P transition (see Fig. 3) is consistent with a change of orientation of the Nb off-center displacement not accompanied by a major change in the absolute value. In particular, from Eq. (13) one deduces an off-center displacement $\lambda \simeq 0.11$ Å at 373 °C and $\lambda \simeq 0.15$ Å at 315 °C.

The numerical values obtained for the Nb displacements in the R and P phase are to be considered only indicative due to the very crude assumptions in the theoretical evaluation of the efg; further refinements are made useless by the present uncertainty in the experimental results. However it is interesting to point out that our data are in good agreement with the earlier conclusions by Lefkowitz et al.[17]

IV. DYNAMICAL EFFECTS

The quadrupole moment of a nucleus affords an excellent probe to study the microscopic dynamics of a crystal near a structural phase transition. In fact the nuclear-spin system is coupled to the lattice through the interaction of the quadrupole moment with the crystalline efg: the large fluctuations in atomic positions occurring near the phase transition are therefore reflected in the spin-lattice relaxation process. Furthermore, since the relaxation is sensitive to the spectral density of the fluctuations in the radiofrequency range, the probe is particularly suitable to study the intensity and the width of the "central peak" of the soft modes. In this section theoretical expressions for the relaxation rate due to rotational motions of the oxygen octahedra are presented and the experimental results are discussed in the light of the theory.

A. Spin-lattice relaxation by rotational motion of the oxygen octahedra

A general review of nuclear spin-lattice relaxation by quadrupole interaction at structural phase transitions can be found in Ref. 18. Here we give the theoretical expressions in a form which directly involves the relevant critical coordinate, i.e., the staggered rotation angle $\varphi_{\vec{q}}$ relative to the motion of the oxygen octahedra. Since the theory will be applied to the case of an intense central component of the soft mode, one can start from the general expression for the relaxation due to a direct process. Any contribution to the relaxation coming from the "normal phonons," which can induce relaxation via a Raman process, is not treated here and is included in the "normal" background relaxation rate.

The relaxation transition probability between Zeeman levels m and $m + \mu$, with $\mu = \pm 1$, ± 2 can be written

$$W_{m,m+\mu} = \frac{1}{\hbar^2} |Q_{\mu m}|^2 \int_{-\infty}^{+\infty} e^{-i\mu\omega_L t} \langle V_\mu(0) V_{-\mu}(t) \rangle \, dt$$

$$= \frac{1}{\hbar^2} |Q_{\mu m}|^2 J(\mu\omega_L) \quad , \tag{14}$$

where $Q_{\mu,m}$ are the matrix elements of the quadrupole-moment operator[19] and

$$V_1 = V_{xz} + i V_{yz} \quad ,$$
$$V_2 = \tfrac{1}{2}(V_{xx} - V_{yy}) + i V_{xy} \quad , \tag{15}$$

with x, y and z Cartesian coordinates in a frame of reference Σ^H defined by $\vec{z} \parallel \vec{H}$. The V_{jk} components are related to the V_{PQ} components in the Σ^C reference frame of the crystal axis by the tensor transformation

$$V_{jk} = \sum_{P,Q} a_j^P a_k^Q V_{PQ} \quad . \tag{16}$$

For a direct relaxation mechanism and in the framework of a classical lattice we can write

$$V_{PQ}(t) = \sum_{l,k} V_{PQ}^{(l,k)} \cong \sum_{l,k} \frac{\partial V_{PQ}^{(l,k)}}{\partial \vec{u}} \cdot \vec{u}(l,k) \quad , \tag{17}$$

where $V_{PQ}^{(l,k)}(t)$ is the contribution from the kth atom in the lth cell and $\vec{u}(l,k)$ is the atomic displacement. The critical atomic motions for the high-temperature phase transitions of $NaNbO_3$ are rotational motions of the oxygen octahedra. Therefore one can consider only the oxygen displacements and can express them in terms of the rotations $\vec{\varphi}_l(t)$ of the oxygen octahedra about the cell center.[20] By doing this one can write

$$V_{PQ}(t) = \sum_{l,k} \frac{\partial V_{PQ}^{(l,k)}}{\partial \vec{u}} \vec{\xi}_k \times \vec{\varphi}_l(t) \quad , \tag{18}$$

where $\vec{\xi}_k$ is a vector connecting the position of the kth oxygen to the Nb atom, i.e., $\vec{\xi}_1 = \tfrac{1}{2} a(1, 0, 0)$, $\vec{\xi}_2 = \tfrac{1}{2} a(0, 1, 0)$, and $\vec{\xi}_3 = \tfrac{1}{2} a(0, 0, 1)$.

Adopting the point-charge approximation for the calculation of the efg one has

$$V_{PQ}(t) = A \sum_l C_l^{PQ} \varphi_l(t) \quad , \tag{19}$$

where $A = 6e(1 - \gamma_\infty)/\sqrt{2} \, a^3$. The C_l^{PQ} coefficients can be easily calculated. The results for the Na^{23},

TABLE I. Coefficients in Eq. (19) for Na^{23} relaxation for rotation around the [001] axis.

PQ \ l	1	2	3	4	5	6
XX	2	−1	−1	−2	−1	−1
YY	−1	−1	2	−1	−1	2
ZZ	−3	0	3	−3	0	3
XY	0	0	0	0	0	0
XZ	0	3	3	0	3	3
YZ	−3	−3	0	−3	−3	0

in the case of rotational motions around the [001] axis, are reported in Table I. The summation has been limited to the eight nearest-neighbor moving oxygen atoms: it involves (see Fig. 9) only three cells in the upper and three cells in the lower (001) plane. For Nb^{93} the summation over the first four nearest-neighbor moving oxygen atoms involves only three cells (cells 1, 2, and 7 in Fig. 9), the only nonzero coefficients are $C_2^{XY} = - C_7^{XY} = 8\sqrt{2}$.

For a rotation around one of the cubic axes the staggered angle $\varphi_{\vec{q}}$ can be written

$$\varphi_{\vec{q}} = \frac{1}{\sqrt{N}} \sum_l e^{-i(\vec{q}+\vec{q}_B)\cdot\vec{R}_l} \varphi_l , \qquad (20)$$

where $\vec{q}_B$ is the wave vector of the zone-boundary mode that drives the phase transition. For a Γ_{25} mode at the R point $\vec{q}_B \equiv (1/a) (\pi, \pi, \pi)$, while for a M_3 mode at the M point $\vec{q}_B \equiv (1/a) (\pi, \pi, 0)$. By substituting Eq. (20) into Eq. (19), and from Eqs. (15) and (16), one can write in the random-phase approximation for the correlation function of V_μ

$$\langle V_\mu(0) V_{-\mu}(t) \rangle = \frac{1}{N} \sum_{\vec{q}} \sum_{PQRS} \Lambda_{PQ}^\mu \Lambda_{RS}^{-\mu} \sum_{11'} C_1^{PQ} C_{1'}^{RS}$$

$$\times \frac{1}{2} A e^{-i(\vec{q}+\vec{q}_B)\cdot\vec{R}_{11'}} \langle \varphi_{\vec{q}}(0) \varphi_{-\vec{q}}(t) \rangle$$

$$\equiv \frac{1}{N} \sum_{\vec{q}} A_{\vec{q}}^\mu \langle \varphi_{\vec{q}}(0) \varphi_{-\vec{q}}(t) \rangle , \qquad (21)$$

where

$$\Lambda_{PQ}^1 = (a_P^x a_Q^z + a_P^y a_Q^z)$$

and

$$\Lambda_{PQ}^2 = \frac{1}{2} (a_P^x a_Q^x + a_P^y a_Q^y) + i a_P^x a_Q^y .$$

The efg components correlation function is therefore expressed as a sum over all $\vec{q}$ values of the correlation function for the staggered angles times a weighting factor $A_{\vec{q}}^\mu$ whose value and $\vec{q}$ dependence are related to the type of coupling, and to
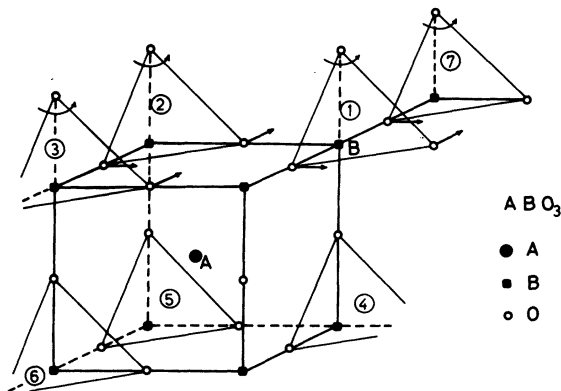

FIG. 9. Cubic perovskite structure and oxygen motion for rotational motions around the [001] axis.

the symmetry of the soft mode. Referring to Table I and taking into account also the analogous results for the rotations around the [100] and [010] axis, it is possible to evaluate the $A_{\vec{q}}^\mu$ factors. In Tables II and III we present the values of $A_{\vec{q}}^\mu$ for the soft modes of interest in $NaNbO_3$ and the $\vec{q}$ dependence of $A_{\vec{q}}^\mu$ in some simple cases. These results will be utilized in the discussion of Sec. IV B.

B. Discussion of the relaxation-rate measurements

In this paragraph our main interpretations will involve the relaxation-rate measurements for the high-temperature phase transitions that can be associated to rotational motions of the NbO_6 octahedra.

In order to discuss the experimental results starting from Eqs. (14) and (21) it is necessary to make assumptions about the $\vec{q}$ and ω dependence of the dynamic form factor

$$S(\vec{q}, \omega) = \int_{-\infty}^{+\infty} \langle \varphi_{\vec{q}}(0) \varphi_{-\vec{q}}(t) \rangle e^{-i\omega t} dt .$$

The phenomenological theory by Schwabl[21] for the critical dynamics of oxygen octahedra, recently integrated by Schneider[22] and supported by the neutron experiments[23] in $SrTiO_3$, indicate the presence in the dynamic form factor $S(\vec{q}, \omega)$ of a central peak in addition to the soft-mode doublet. The neutron-scattering experiments give some indication about the $\vec{q}$ width and the frequency width of the central peak near T_c. EPR measurements by von Waldkirch et al.[24] indicate that the frequency width of the central peak for $\vec{q}$ close to the critical $\vec{q}$ value $\vec{q}_c$ reaches the radiofrequency range at about 1 °C from T_c. Since the nuclear spin-lattice relaxation rate probes the spectral density of the local rotation-angle fluctuations (i.e., integrated over all $\vec{q}$ values) for very low frequency, T_1^{-1} should be very sensitive to the presence of a central peak.

In the neighborhood of the transition we can assume[21] that the low-frequency part of the power spectrum is well described by a Lorenzian shape

$$S(\vec{q}, \omega) = \langle | \varphi_{\vec{q}} |^2 \rangle [2\Gamma_{\vec{q}}/(\Gamma_{\vec{q}}^2 + \omega^2)] , \qquad (22)$$

which corresponds to an exponential decay of the correlation function at long time, i.e., $\langle \varphi_{\vec{q}}(0) \varphi_{-\vec{q}}(t) \rangle = \langle | \varphi_{\vec{q}} |^2 \rangle e^{-\Gamma_{\vec{q}} t}$. From the fluctuation-dissipation theorem and Kramers-Kronig relations $\langle | \varphi_{\vec{q}} |^2 \rangle = kT\chi(\vec{q}, 0)$, therefore we can write, for the relaxation rate

$$W_{m, m+\mu} = \frac{1}{\hbar^2} | Q_{m\mu} |^2 \frac{2kT}{N} \sum_{\vec{q}} A_{\vec{q}}^\mu \frac{\chi(\vec{q}, 0) \Gamma_{\vec{q}}}{(\mu\omega_L)^2 + \Gamma_{\vec{q}}^2} . \qquad (23)$$

The $\omega = 0$ generalized collective susceptibility $\chi(\vec{q}, 0)$ and the quantity $\Gamma_{\vec{q}}$ have a temperature de-

TABLE II. $A_{\vec{q}}^{\mu}$ factors in perovskite ABO_3 structure for wave vectors at the zone boundary ($\vec{q}_B = (\pi/a)$, (π/a), q_{Bz}). $F(\alpha, \beta, \gamma) = \frac{1}{3}(\frac{1}{2} \sin^2 2\beta \cos^2 2\gamma + \sin^2 2\beta + \frac{3}{2} \sin^2 2\gamma)$; $G(\alpha, \beta, \gamma) = \frac{1}{12}(6 \sin^4\beta - 4 \sin^2\gamma\sin^4\beta + 2 \sin^4\beta\sin^4\gamma - 6 \sin^2\beta + 6)$; α, β, γ: Euler angles for the orientation of Σ^C with respect to Σ^H; for a point charge model, nearest-neighbors interaction: $E = 144e^2(1 - \gamma_\infty)^2/a^6$.

	$A_{\vec{q}_B}^1$	$A_{\vec{q}_B}^2$	
Single crystal	$(1 + \cos q_{Bz}a)F(\alpha, \beta, \gamma)E$	$(1 + \cos q_{Bz}a)G(\alpha, \beta, \gamma)E$	A site
Powder	$(1 + \cos q_{Bz}a)\frac{17}{36}E$	$(1 + \cos q_{Bz}a)\frac{17}{45}E$	
Single crystal	0	0	B site
Powder	0	0	

pendence characterized by a singular behavior for the components at $\vec{q}$ close to $\vec{q}_c$ and for $T \rightarrow T_c$, which corresponds to a narrowing and an increase of intensity of the central peak.

From Eq. (23) we observe that the relaxation rate measures the spectral-density component at ω_L or $2\omega_L$ of all the $\vec{q}$ components of the central peak weighed by the $A_{\vec{q}}^{\mu}$ factor. If the $A_{\vec{q}}^{\mu}$ factor is different from zero for $\vec{q} = \vec{q}_c$, the relaxation rate exhibits a critical behavior for $T \rightarrow T_c$, which measures the increase in intensity of the $\vec{q}$ integrated central peak at the Larmor frequency. On the other hand, if the $A_{\vec{q}}^{\mu}$ factor is zero, it is expected that the critical enhancement of the central peak, on approaching T_c, shows up very little in the T_1 measurements. The presence of the weighing factor $A_{\vec{q}}^{\mu}$ in the formula for the relaxation rate reflects the fact that this quantity is sensitive to both the autocorrelation and the pair-correlation functions for the local rotational angles of the cells nearest neighbors to the nucleus whose relaxation is being considered. Consequently, the mere presence or lack of a critical contribution to the relaxation rate can give information about the symmetry properties of the soft modes or, in other words, of the correlation properties of the rotational fluctuations.

Let us refer to the highest-temperature phase

transition in $NaNbO_3$ at 641 °C. As it appears from Figs. 6 and 7, a critical contribution to the relaxation rate is present for Na^{23} but not for Nb^{93}. An inspection of Table II allows an immediate explanation of the lack of critical contribution in the Nb^{93} relaxation rate. In fact at the Nb site $A_{\vec{q}}^{\mu} = 0$ for any wave vector at the zone boundary, independently from q_{Bz}. In other words, the rotational motions of the oxygen octahedra are ineffective in producing relaxation at the Nb site, irrespective of the correlation properties between adjacent planes perpendicular to the rotation axis.

The presence of a critical contribution in the Na^{23} relaxation rate indicates that the $A_{\vec{q}_c}^{\mu}$ factor at the Na site must be different from zero. From Table II it can be seen that $A_{\vec{q}_c}^{\mu} = 0$ for $\vec{q}_c$ at the R point (i.e., $q_{Bz} = \pi/a$), while $A_{\vec{q}_c}^{\mu}$ is different from zero from a M_3 mode (i.e., $q_{Bz} = 0$). It is also possible that the softening involves all the branch from R to M. The softening of the M_3 mode corresponds to a tridimensional correlation with rotations of successive oxygen octahedra along the z axis (e.g., octahedra 3 and 6 in Fig. 9) in the same sense, while the softening of the whole branch from R point to M point corresponds to rotational fluctuations two-dimensionally correlated within (001) planes and without correlation between adjacent planes. In this case the $A_{\vec{q}}^{\mu}$ factor would be an average obtained by integrating over q_{Bz} the expression in Table II; this yields $A_{\vec{q}_M-R}^{\mu} = \frac{1}{2}A_{\vec{q}_M}^{\mu}$.

Concluding, the 641°C cubic-tetragonal phase transition must involve softening of the M_3 mode or of a large part of the M-R branch. The anisotropic diffuse x-ray scattering[3,6] observed in $NaNbO_3$ at $T > 641$ °C is in favor of a flat dispersion for the R-M branch.

It is useful at this point to comment on the results obtained[25] for the Sr^{83} relaxation rate in $SrTiO_3$ above the 105 °K structural phase transition. The measurements were performed in a single crystal. Since no critical effect was observed in T_1^{-1} for different crystal orientations, it can be concluded that the transition involves the

TABLE III. $\vec{q}$ dependence for the $A_{\vec{q}}^{\mu}$ factors.

	$A_{\vec{q}}^1$	$A_{\vec{q}}^2$
A site—single crystal (only for a cubic axis along H_0)	$3E[\cos(q_{Bx}+q_z)a+1]$ $\times [2 - \cos q_x a - \cos q_y a]$	$\frac{1}{8}E[\cos(q_{Bx}+q_z)a+1][39-13$ $\times \cos(q_x - q_y)a - 11\cos q_x a - 11\cos q_y a]$
B site—single crystal (generic orientation)	$\frac{32}{3}E[1 - \cos(q_x - q_y)a]$ $\times [\frac{1}{16}\sin^2 2\beta \sin^2 2\gamma + \sin^2\beta$ $\times \sin^4\gamma + \cos^4\beta + \cos^2\beta]$	$\frac{8}{3}Ec(\alpha, \beta, \gamma)$ $\times [1 - \cos(q_x - q_y)a]$
B site—powder	$\frac{128}{15}E[1 - \cos(q_x - q_y)a]$	$\frac{16}{27}E[1 - \cos(q_x - q_y)a]$

softening of the Γ_{25} mode $(q_{Bz} = \pi/a)$, which corresponds to three-dimensional correlations of the rotational fluctuations. This conclusion agrees with the absence of anisotropic diffuse intensity in the electron diffraction[6] in $SrTiO_3$, in contrast with $NaNbO_3$.

Referring again to the $NaNbO_3$ measurements, there is no critical contribution to the Na^{23} relaxation rate (see Fig. 6) at the phase transition which occurs at 575 °C, involving rotational displacements from $a^0a^0c^+$ to $a^-b^0c^+$. In the tetragonal T_2 phase above 575 °C the rotations of the oxygen octahedra around the three pseudocubic axes are no longer equivalent. Also, the transition is associated to a rotational displacement around an axis perpendicular to the $\bar{c}$ tetragonal axis with the opposite sense in adjacent planes perpendicular to the $\bar{c}$ axis, i.e., freezing of a Γ_{25}-type mode at the R point.[5] The situation is then similar to $SrTiO_3$ and the lack of critical contribution to the Na^{23} relaxation rate is consistent with the above description of the transitions.

The T_1-S phase transition is not very well understood in terms of tiltings of the oxygen octahedra. There is speculation[5] that the phase S is characterized by a tilted system with some pairs of (010) layers described by $a^-b^+c^+$ and some described by $a^-b^0c^+$. It seems to be difficult to describe the dynamics of this transition in terms of a freezing of a particular rotational mode. But it can be observed that the small anomalous behavior of the Na^{23} relaxation rate (see Fig. 6) is consistent with a M_3 type mode corresponding to rotations around the [010] pseudocubic axis and support the above hypothesis for the tilted system of the S phase.

V. TEMPERATURE DEPENDENCE OF THE Na^{23} RELAXATION RATE

In the preceding discussion we limited ourselves to the information involving the symmetry of the soft modes which can be deduced from the presence of or lack of a critical contribution to the relaxation rate at $T \rightarrow T_c$. In the following discussion we will consider in more detail the temperature behavior of the relaxation rate on approaching T_c from the high-temperature side. Let us consider the Na^{23} relaxation rate near the 641 °C phase transition. In this case the factor $A^\mu_{\vec{q}_c}$ is different from zero. In order to obtain the temperature dependence of the relaxation rate, one should perform a sum over $\vec{q}$ of the critical quantities $\chi(\vec{q}, 0)$ and $\Gamma_{\vec{q}}$ weighed by the $A^\mu_{\vec{q}}$ factor according to Eq. (23). This calculation can be extremely cumbersome. It is possible, however, to simplify the problem by neglecting the $\vec{q}$ dependence $A^\mu_{\vec{q}}$ and by substituting in Eq. (23) for $A^\mu_{\vec{q}}$ the constant value $A^\mu_{\vec{q}_c}$. In fact, it can be argued that the main contributions to the summation over $\vec{q}$ in Eq. (23)

come from the terms with $\vec{q}$ close to $\vec{q}_c$, because for these terms the amplitude of the fluctuations is larger and the power spectrum is concentrated in the low-frequency region. With this simplification, the sum over all $\vec{q}$ values can be evaluated in the assumption of "fast motions" (i.e., $\Gamma_{\vec{q}} > \omega_L$ for every $\vec{q}$) and by putting

$$\Gamma_{\vec{q}}^{-1} \propto \chi(\vec{q}, 0) \propto [q^2 - (1 - \Delta)q_z^2 + k^2]^{-1 + \eta/2} \quad , \qquad (24)$$

as follows from Schwabl[21] theory. Here k is the inverse of the correlation length and Δ is an anisotropy parameter which is $\Delta = 1$ for three-dimensionally correlated rotations and $\Delta = 0$ for two-dimensionally correlated rotations. The $\vec{q}$ is measured starting from the wave vector $\vec{q}_M$ at the zone boundary $(\pi/a, \pi/a, 0)$. The result for the critical contribution to the Na^{23} relaxation rate in a powder can be written, from Eqs. (6), (23), and (24),

$$\frac{1}{T_1} = \frac{2}{5}\left(\frac{17}{36} + 4\frac{17}{45}\right)\frac{e^2Q^2}{12\hbar^2}\frac{288e^2(1 - \gamma\infty)^2}{a^6}\frac{\langle\varphi_0^2\rangle k_0^4}{\Gamma_0}$$

$$\times\frac{1}{N}\sum_{\vec{q}}\frac{1}{[q^2 - (1 - \Delta)q_z^2 + k^2]^{-1 + \eta/2}} \, , \qquad (25)$$

where the numbers $\frac{17}{36}$ and $\frac{17}{45}$ come from averaging over the Euler angles the functions F and G in Table II. We have also assumed $k = k_0\epsilon^\nu$, $\Gamma_{qc} = \Gamma_0\epsilon^\gamma$ and $\langle |\varphi_{\vec{q}_c}^2|^2\rangle = \langle\varphi_0^2\rangle\epsilon^{-\gamma}$ with $\gamma = (2 - \eta)\nu$.

Transforming the sum over $\vec{q}$ to an integration over the Debye sphere, for the leading term in the temperature dependence of the critical contribution, the result is (for $\epsilon \leq 5\times 10^{-1}$)

$$\frac{1}{T_1} \propto \frac{k^{-1 + 2\eta}}{\sqrt{\Delta}}\arctan\frac{\pi\sqrt{\Delta}}{ka} \quad , \qquad (26)$$

which, for three-dimensional correlation $(\Delta = 1)$, reduces to

$$(1/T_1) \propto k^{-(1 - 2\eta)} \propto \epsilon^{-\nu(1 - 2\eta)} \quad (\text{for } ka \ll 1), \qquad (27)$$

while for two-dimensional correlations $(\Delta = 0)$ the result is

$$(1/T_1) \propto k^{-2(1 - 2\eta)} \propto \epsilon^{-2\nu(1 - \eta)} \quad . \qquad (28)$$

The experimental results for the Na^{23} relaxation rate are plotted in Fig. 10 in a double logarithmic plot. In no temperature interval is a straight line obtained. This rules out the validity of either of the two extreme cases illustrated by Eqs. (27) and (28). The best fit of the experimental data according to Eq. (26) (where we set $\eta = 0$) yields $\nu \simeq 0.6$ and $\frac{1}{100} \leq \Delta \leq \frac{1}{50}$. These values agree well with the results for the critical exponents[26] at structural phase transitions and with the indication of the two-dimensional-type correlation of the fluctuations.[3,6] However, we believe that they cannot be taken too seriously. In fact, the fit of the experimental data can be misleading when one considers that differ-
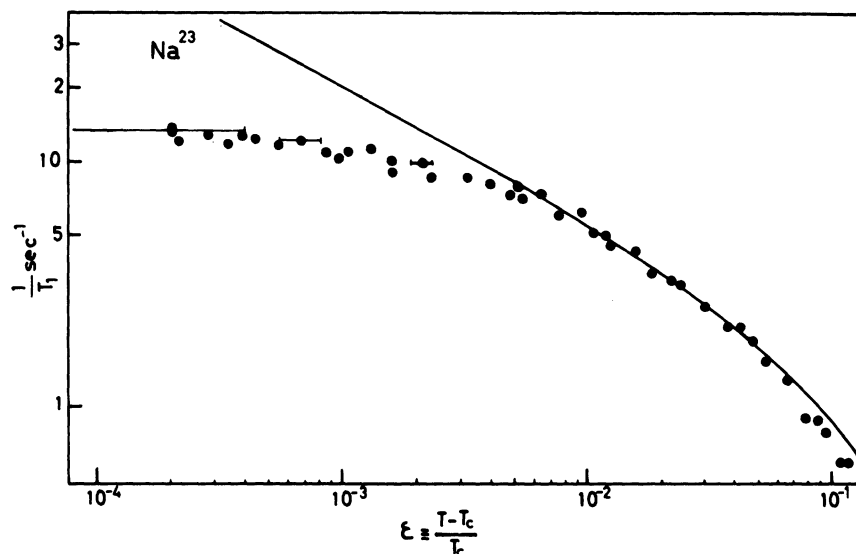
FIG. 10. Log-log plot of the critical contribution to the Na^{23} spin-lattice relaxation rate near the 641 °C transition as a function of ϵ. Solid line is the best-fit theoretical behavior according to Eq. (26) in the text and corresponds to the value $\nu = 0.6$ and $\Delta = \frac{1}{50}$. A background contribution of 1 sec^{-1} has been subtracted.

ent effects could influence the temperature dependence of the relaxation rate. Besides the choice of the adjustable parameters ν and Δ, there can be a frequency effect as $T \to T_c$ (i. e., changeover from fast- to slow-motion regime) and an effect due to the $\vec{q}$ dependence of the $A_{\vec{q}}^{\mu}$ factor at T far from T_c. We will briefly discuss this in the following.

Below $\epsilon \simeq 5 \times 10^{-3}$ the theoretical expression of Eq. (26) cannot fit the experimental results for any acceptable value of ν and Δ. Most probably in this temperature range the "fast-motion" approximation ceases to be valid and it is necessary to retain the resonance frequency term $\mu \omega_L$ in the evaluation of the relaxation rate from Eq. (23). In this case a very complicated expression for the relaxation rate is obtained. The main feature which appears in the expression is that very close to T_c (when the frequency of the critical motions become lower than ω_L) a flattening of the relaxation rate occurs. The qualitative explanation for this flattening is that the lowering of the frequency of the collective motions under ω_L, that would cause the relaxation rate to reduce as $\Gamma_{\vec{q}}^-$ [see Eq. (23)] is compensated by the increase in amplitude of the collective motions. The indication that the width $\Gamma_{\vec{q}_c}$ of the central peak becomes of the order of the Larmor frequency is supported by the comparison with the EPR results[24] in $SrTiO_3$. For this crystal, accurate measurements of EPR linewidth of substitutional Fe^{3+} ions were performed as a function of temperature around the 105 °K transition. In the fast-motion regime the EPR linewidth is proportional to the spectral density of the local rotational fluctuations at zero frequency, and consequently, it gives the same information as the nuclear spin-lattice relaxation rate. In the measurements of linewidth a changeover from the fast-motion to.

the slow-motion regime occurs approximately when $\Gamma_{\vec{q}_c}$ becomes of the order of the linewidth itself. From this consideration it can be deduced, for $SrTiO_3$, $\Gamma_{\vec{q}_c} \simeq 2\pi$ 70 MHz at $\epsilon \simeq 7 \times 10^{-3}$. Since for spin-lattice relaxation measurements a frequency effect should be felt when $4\pi\nu_L \simeq \Gamma_{\vec{q}_c}$, it can be seen that for $\nu_L = 22$ MHz it is possible that a frequency effect is present in our measurements near T_c.

An advantage of spin-lattice relaxation measurements over linewidth measurements is that by changing the resonance frequency one can, in principle, probe the width of the central peak at different temperatures and the shape in frequency at a given temperature. Unfortunately, in $NaNbO_3$ the poor signal-to-noise ratio prevents a significant lowering in the resonance frequency. However, it is possible to perform measurements of the spectral density at almost zero frequency by measuring the relaxation rate in the rotating frame. This type of measurement, which is presently under way, has in addition the advantage that the temperature behavior very close to T_c should allow a direct determination of the critical index ν.

The expression of Eq. (26) which we have utilized to fit the experimental data was obtained by approximating $A_{\vec{q}}^{\mu} = A_{\vec{q}_c}^{\mu}$. We have investigated in a particular case the effect of retaining the correct $\vec{q}$ dependence of $A_{\vec{q}}^{\mu}$ on the temperature dependence of the relaxation rate. For a single crystal with $\Sigma^C \equiv \Sigma^H$, taking into account the results in Table III, from Eqs. (23) and (24) we obtain

$$W_2 \propto I \left(1 - 5.7\, a^2 k^2 \right) \ , \tag{29}$$

where I represents the critical contribution of Eq. (26). Since $k_0 \simeq a^{-1}$, $a^2 k^2 \simeq \epsilon^{2\nu}$, and Eq. (29) shows that with $\nu = 0.6$ the correction is practically negligible only for $\epsilon \lesssim 4 \times 10^{-2}$.

VI. TEMPERATURE DEPENDENCE OF THE Nb^{93} RELAXATION RATE

The lack of a sizeable critical contribution to the Nb^{93} relaxation rate for the three high-temperature transitions has already been justified from the consideration that at the Nb site $A_{\vec{q}_c}^{\mu} = 0$ for any $\vec{q}$ at the zone boundary. On the other hand, the relaxation rate (see Fig. 7) shows an unusual constancy over the whole temperature range 520–800 °C (in the ordinary quadrupole spin-phonon relaxation $W \propto T^2$).

Since the $\vec{q}$ dependence of $A_{\vec{q}}^{\mu}$ at the Nb site has a simple form (see Table III), the Nb^{93} relaxation rate can be evaluated in close form if a reliable expression of $\chi(\vec{q}, 0)$ for the whole Brillouin zone was available. Using for $\chi(\vec{q}, 0)$ the expression (24), it is possible to obtain an expression for the Nb^{93} relaxation rate coming from the $\vec{q}$ values close to $\vec{q}_c$. For a powdered crystal, from Eqs. (8) and (23), and from Table II, by integrating in cylindrical coordinates, we obtain, in the fast-motion regime,

$$\frac{1}{T_1} = \frac{e^2 Q^2}{540\,\hbar^2}\; \frac{256\,e^2(1-\gamma\infty)^2}{a^6}\; \frac{184}{15}\; \frac{\langle\varphi_0^2\rangle k_0^4}{\Gamma_0}\; \frac{a^2}{8\pi^2 N}$$

$$\times \left(\frac{q_m^2(2-\sqrt{\Delta})+2k^2}{\Delta(q_m^2+k^2)^{1/2}}\; \arctan\; \frac{\pi\sqrt{\Delta}}{a(q_m^2+k^2)^{1/2}} \right.$$

$$\left. -4k\; \arctan\; \frac{\pi\sqrt{\Delta}}{ak} + \frac{\pi}{a}\log\frac{\pi^2\Delta+q_m^2a^2+k^2a^2}{\pi^2\Delta+k^2a^2} \right) ,$$

$$(30)$$

where q_m is the maximum q value for which the anisotropic Orstein-Zernike expression[24] for $\chi(\vec{q}, 0)$ can be assumed valid. This expression, apparently very complicated, results in a relaxation rate which for $\Delta \leqslant \frac{1}{50}$ is practically temperature independent, in good agreement with the experimental results.

Incidentally, the lack of a critical contribution to the Na^{23} relaxation rate in the neighborhood of the tetragonal-orthorhombic transition at 575 °C (where the $A_{\vec{q}_c}$ factor is zero) can be explained in a similar way.

VII. DISCUSSION OF THE ORDERS OF MAGNITUDE

The numerical calculation of the relaxation rate according to Eqs. (25), (26), and (30) requires the knowledge of the quantities $\langle\varphi_0^2\rangle$, k_0, and Γ_0 for which no reliable values are available. However, to check the validity of the expressions for the relaxation rate it is possible to compare the theoretical and experimental ratios R of the Na^{23} and Nb^{93} relaxation rates. The agreement is good in the entire temperature range, with the exception of the region in which the frequency effect is felt and Eq. (26) is no longer valid. For example, at $\epsilon = 10^{-1}$

$R_{theor} = 0.046$ to be compared with $R_{exp} = 0.042$. In the evaluation of R_{theor} we used the values of $\Delta = \frac{1}{50}$ and $\nu = 0.6$ obtained from the fitting of the Na^{23} relaxation rate and $k_0 = 0.23$ Å^{-1} as in $SrTiO_3$, as indicated by neutron measurements.[27] Since the agreement between theory and experiment is encouraging, we can derive an estimate for the quantity $\langle\varphi_0^2\rangle/\Gamma_0$ from the experimental value of the relaxation rate. One finds from either the Na^{23} or the Nb^{93} relaxation rate for T around T_c a value $\langle\varphi_0^2\rangle/\Gamma_0 = 2\times10^{-14}$ (sec rad^2).

No indication exists in the literature about the value of Γ_0. An approximate value can be obtained from our data. By examining the deviation of the experimental points from the theoretical fit in Fig. 10, we can set $\Gamma_{\vec{q}_c} \simeq 2\omega_L = 2.8\times10^8$ Hz at approximately $\epsilon \simeq 4\times10^{-3}$. By assuming $\Gamma_{\vec{q}_c} = \Gamma_0\epsilon^{\gamma}$ and $\gamma = 1.2$, we can deduce $\Gamma_0 = 2\times10^{11}$. This value of Γ_0 would lead to $\langle\varphi_0^2\rangle \simeq 4\times10^{-3}$ rad^2 which corresponds to $\langle\varphi_0^2\rangle^{1/2} \simeq 3.5°$.

If an indication concerning the amplitude of the fluctuating local angle around T_c is desired, it can be assumed that

$$\langle\varphi_{loc}^2\rangle = \frac{1}{N}\sum_{\vec{q}}\langle|\varphi_{\vec{q}}|^2\rangle .$$

By assuming $\langle|\varphi_{\vec{q}c}|^2\rangle = \langle\varphi_0^2\rangle\epsilon^{-\gamma}$, $k = k_0\epsilon^{\nu}$ and $2\nu = \gamma$, and by performing the summation, the result at T_c is

$$\langle\varphi_{loc}^2\rangle^{1/2} \simeq 0.5\langle\varphi_0^2\rangle^{1/2} = 1.75° .$$

The mean spread of the local rotational displacement for $NaNbO_3$ is larger than the one estimated for $SrTiO_3$.[28] Also, the maximum static rotation angle is larger (near 7°) in $NaNbO_3$ (see Fig. 4) than for $SrTiO_3$,[15] where it is only about 2°.

Finally, the temperature dependence of the Nb^{93} relaxation rate in the neighborhood of the antiferro- and ferroelectric phase transitions involve the off-center motion of Nb atoms. A discussion of the Nb^{93} relaxation rate due to off-center motion has been presented in connection with the ferroelectric phase transitions in $KNbO_3$.[18] The main conclusion that can be drawn from the lack of critical contribution at the ferro- and antiferroelectric phase transitions is that the softening of the branches along the [100] directions involve only the small $\vec{q}$ values.

ACKNOWLEDGMENTS

APPENDIX

Let us consider a system of identical spins I, in the rotating frame; if the spin system is subjected to a secular magnetic dipolar or electric quadrupolar perturbation $\hbar\mathcal{K}'$ ($[\mathcal{K}', I_z] = 0$) the Hamiltonian can be written

$$\hbar\mathcal{K} = -\gamma\hbar H_1 I_y + \hbar\mathcal{K}' \quad,$$

where $I_y = \sum_i I_y^i$.

The fp decay after a rf pulse of duration τ is given by[19]

$$h_+(t) \propto \mathrm{Tr}\left[e^{-i\mathcal{K}'t}\rho(\tau)\,e^{i\mathcal{K}'t}\,I_+\right] \quad, \tag{A1}$$

where

$$\rho(\tau) = e^{-i\mathcal{K}\tau}\,I_z\,e^{i\mathcal{K}\tau} \quad. \tag{A2}$$

Usually one neglects the effect of the interaction $\mathcal{K}'$ during the pulse, and consequently for a $90°$ pulse ($\gamma\mathcal{K}_1\tau = \frac{1}{2}\pi$) one has

$$h_+(t) \propto \mathrm{Tr}\left(e^{-i\mathcal{K}'t}I_x\,e^{i\mathcal{K}'t}I_+\right) \quad. \tag{A3}$$

By taking into account the interaction $\mathcal{K}'$ also during the pulse, one can obtain,[29] in a first-order approximation,

$$h_+(t) \propto \mathrm{Tr}\left(e^{-i\mathcal{K}'(t+t_1)}I_x\,e^{i\mathcal{K}'(t+t_1)}I_+\right) \quad, \tag{A4}$$

which is valid in the following cases.

(i) $\mathcal{K}' = -\sum_i u_i I_z^i$; i.e., spread of the resonance frequencies by local magnetic fields due to the dipole moments of nonresonant nuclei or electrons. The above Hamiltonian also describes, in the framework of the fictitious spin-$\frac{1}{2}$ formalism, the broadening of the central line by a second-order quadrupole interaction in a powdered crystal. In these cases, one has

$$\rho(\tau_{\pi/2}) = \sum_i\left(I_x^i - \frac{u_i}{\gamma H_1}I_y^i\right) \quad,$$

from which one obtains $t_1 = 1/\gamma H_1 = (2/\pi)\,\tau_{\pi/2}$.

(ii) $\mathcal{K}' = \sum_{i>j} b_{ij}(3 I_z^i I_z^j - \underline{I}^i \cdot \underline{I}^j)$; i.e., the line broadening is due to the dipole-dipole interaction between the resonant nuclei. In this case one has

$$\rho(\tau_{\pi/2}) = \sum_i I_x^i - \frac{\pi}{4}\sum_{i>j}\frac{b_{ij}}{\gamma H_1}(I_y^i I_z^j + I_z^i I_y^j)$$

and[30]

$$t_1 = \tfrac{1}{4}\pi\gamma H_1 = \tfrac{1}{2}\tau\pi \quad.$$

(iii) $\mathcal{K}' = \sum_i a_i(I_z^i)^2$; i.e., first-order quadrupole broadening of the satellite lines. In this case one has

$$\rho(\tau_{\pi/2}) = \sum_i\left(I_x^i - \frac{\pi}{4}\frac{a_i}{\gamma H_1}(I_x^i I_z^i + I_z^i I_x^i)\right)$$

and again

$$t_1 = \tfrac{1}{4}\pi\gamma H_1 \quad.$$

By a comparison of Eqs. (A3) and (A4) one obtains that, even if the rf field intensity is not very high, the fp decay is again the Fourier transform of the frequency distribution, provided one takes the origin of the time not at the end of the pulse but at a time t_1 before. A check of the limits of validity of the time-translation correction has been performed[29] by evaluating the shape of the fp decay in the case of a Gaussian distribution of local magnetic field [case (i)], where a classical picture is possible. It has been proved that the time-translation correction retains its substantial validity until a value of rms width of the frequency distribution $M_2^{1/2}$ of the order of $\frac{1}{2}(1/2\pi)\gamma H_1$.

[1]As general reference on perovskite compounds, see A. M. Glazer, Acta Crystallogr. B **28**, 3384 (1972).

[2]H. D. Megaw, J. Phys. (Paris) **33**, C2-1 (1972).

[3]F. Denoyer, R. Comés, and M. Lambert, Acta Crystallogr. A **27**, 414 (1971).

[4]A. M. Glazer and H. D. Megaw, Philos. Mag. **25**, 1119 (1972).

[5]M. Ahtee, A. M. Glazer, and H. D. Megaw, Philos. Mag. **26**, 995 (1972).

[6]K. Ishida and G. Honjo, J. Phys. Soc. Jap. **34**, 1279 (1973).

[7]F. Wolf, D. Kline, and H. S. Story, J. Chem. Phys. **53**, 3538 (1970).

[8]G. Bonera, F. Borsa, and A. Rigamonti, J. Phys. (Paris) **33**, C2-195 (1972).

[9]G. Bonera, F. Borsa, and A. Rigamonti, *Magnetic Resonance and Related Phenomena*, edited by V. Hovi (North-Holland, Amsterdam, 1973), p. 50.

[10]G. Bonera, F. Borsa, M. L. Crippa, and A. Rigamonti, Phys. Rev. B **4**, 52 (1971); see also Phys. Rev. **165**, 391 (1968).

[11]R. E. Walstedt, Phys. Rev. B 5, 41 (1972).

[12]K. Kambe and J. F. Ollom, J. Phys. Soc. Jap. **11**, 50 (1956).

[13]A. Avogadro and A. Rigamonti, in Ref. 9, p. 255.

[14]It should be noted that a small peak at 660 °C seemed to appear even in sample II after several heating and cooling cycles. This effect suggests that whatever may be the cause for the extra peak at 660°C, it is introduced with the aging of the sample.

[15]K. A. Müller and W. Berlinger, Phys. Rev. Lett. **26**, 13 (1971).

[16]F. Borsa, Phys. Rev. B **7**, 913 (1973).

[17]I. Lefkowitz, K. Lukaszewicz, and H. D. Megaw, Acta Crystallogr. 20, 670 (1966).

[18]G. Bonera, F. Borsa, and A. Rigamonti, Nuovo Cimento **2**, 325 (1972).

[19]A. Abragam, *Principles of Nuclear Magnetism* (Oxford U. P., Oxford, England, 1961).

[20]E. Pytte and J. Feder, Phys. Rev. **187**, 1077 (1969).

[21]F. Schwabl, Phys. Rev. Lett. **28**, 500 (1972).

[22]T. Schneider, Phys. Rev. B **7**, 201 (1973).

[23]S. M. Shapiro, J. D. Axe, G. Shirane, and T. Riste, Phys. Rev. B **6**, 4332 (1972).

[24]Th. von Waldkirch, K. A. Müller, and W. Berlinger, Phys. Rev. B **7**, 1052 (1973).

[25]A. Angelini, G. Bonera, and A. Rigamonti, in Ref. 9, p. 346.

[26]In fact, for the 105 °K phase transition in $SrTiO_3$ a value of $\nu = 0.65$ is reported (Ref. 24); in addition ν should be equal to 2β and a value $\beta = 0.33$ for the rotational order parameter was found in $LaAlO_3$ and $SrTiO_3$ (Ref. 15) and in $KMnF_3$ (Ref. 16).

[27]T. Riste, E. J. Samuelsen, K. Otnes, and J. Feder, Solid State Commun. **9**, 1455 (1971); see also Ref. 23.

[28]K. A. Müller, *Proceedings of the NATO Advanced Study Institute on Anharmonic Lattices, Structural Transitions and Melting, Geilo, Norway,* 1973, edited by T. Riste (Plenum, to be published).

[29]C. I. Massara, thesis (Università di Pavia, 1972) (unpublished).

[30]This result has already been found by D. E. Barnall and I. J. Lowe, Phys. Rev. **148**, 328 (1966).